Tree-ring width and blue intensity chronologies of three co-existing conifer species from the Russian Altai mountains reveal different climate signals

Alberto Arzac[1], Alexander V. Kirdyanov[1,2], Viktoria Agapova[1], Alina A. Kirdyanova[3], Daniel Diaz de Quijano[1,4], Nikolay I. Bykov[5], Ulf Büntgen[6,7,8]

[1] Siberian Federal University, Krasnoyarsk 660041, Russia

[2] V.N. Sukachev Institute of Forest SB RAS, Federal Research Center "Krasnoyarsk Science Center SB RAS", Krasnoyarsk, Russia

[3] Institute of Earth Science, Saint-Petersburg State University, Saint-Petersburg 199034, Russia

[4] Departament de Biologia Evolutiva, Ecologia i Ciències Ambientals, Universitat de Barcelona, Barcelona 08028, Catalonia

[5] Institute for Water and Environmental Problems SB RAS, Barnaul 656038, Russia

[6] Department of Geography, University of Cambridge, Cambridge, UK

[7] Global Change Research Centre (CzechGlobe), Brno, Czech Republic.

[8] Department of Geography, Faculty of Science, Masaryk University, Brno, Czech Republic.

Corresponding author: Alberto Arzac, aarzac@gmail.com +7 (902) 979 96 95

Abstract

The Altai in southern Siberia is one of the few mountain ranges at mid-latitudes from where summer temperatures have been reconstructed over the past 2,000 years. While tree-ring width (TRW) measurements have been used traditionally, the paleoclimatic potential of more advanced wood density parameters from different tree species remains widely unexplored in this region. Here, we examine the climate response of three co-existing conifer species (*Larix sibirica* Ledeb., *Pinus sibirica* Du Tour and *Picea obovata* Ledeb.) from the Russian Altai at ~1600 m asl. We develop TRW, latewood blue intensity (LWBI), and delta blue intensity (DBI) chronologies, and compare these against monthly temperature means and precipitation totals over the 1951–2021 period. Our results show that all three species respond positively to summer temperatures. The LWBI and DBI chronologies exhibit stronger and more consistent summer temperature signals compared to TRW, with the highest correlations exhibited by *P. obovata* (r = 0.7) and *P. sibirica* (r = 0.5). Despite species-specific differences in temperature sensitivity, our findings demonstrate the potential of LWBI and DBI for robust reconstructions of summer temperature in inner Eurasia.

Keywords: dendroclimatology, global warming, mixed forest, tree growth, temperature reconstructions

1. Introduction

Over the last century, the Altai mountains, a region spanning Russia, China, Mongolia, and Kazakhstan, have experienced significant warming (Bezuglova et al., 2012; Cazzolla Gatti et al., 2019). Rapid warming has impacted snowmelt patterns, hydrological regimes and vegetation distribution (Blyakharchuk et al., 2004; Cazzolla Gatti et al., 2019, 2018; Mukhanova et al., 2016). The Altai has been a focal point for dendrochronological studies aiming at identifying growth-climate relationships at tree-ring and anatomical levels (Barinov et al., 2016; Bykov et al., 2023; Fonti et al., 2013; Jiang et al., 2021; Shah et al., 2023; Tainik et al., 2015; Wang et al., 2023; Zhou et al., 2021). The combination of multiparametric approaches such as latewood maximum density and tree growth modeling provide further insight into tree growth variability under changing climate (Chen et al., 2012; Churakova (Sidorova) et al., 2022; Kang et al., 2022; Kirdyanov et al., 2024a; Sidorova et al., 2012).

The Altai mountains are among the few mid-latitude regions where millennial-long tree-ring width chronologies have been developed to reconstruct past summer temperature variability (Büntgen et al., 2016; Davi et al., 2021; Mukhanova et al., 2016; Myglan et al., 2008, 2012, 2015; Ovtchinnikov et al., 2000; Sidorova et al., 2013). However, while TRW is widely used as a proxy for summer temperature, its signal can be influenced by non-climatic factors and biological memory (Barchenkov et al., 2023; Büntgen et al., 2020; Esper et al., 2007, 2015; Fritts, 1976). In contrast, maximum latewood density (approximated by blue intensity), is generally more directly related to summer temperature fluctuations and less affected by non-climatic influences (Esper et al., 2002, 2016).

The high mountain taiga in the Altai, between 700 and 2100 m a.s.l. (Blyakharchuk et al., 2004), harbors a diverse range of tree species, including *Larix sibirica* Ledeb. (Siberian larch), *Pinus*

sibirica Du Tour (Siberian pine), and *Picea obovata* Ledeb. (Siberian spruce). Each of these species exhibits unique physiological and ecological traits that shape their resilience and adaptability to climatic variability. *L. sibirica*, is a shade-intolerant and drought-resistant species, thriving under extreme low temperatures (Abaimov, 2010; Tchebakova et al., 2016). As a pioneer species, it is among the first to colonize disturbed, open environments (Gower and Richards, 1990). Unlike the other two species, *L. sibirica* is a deciduous conifer, shedding its needles in winter to reduce water loss as an adaptation to extreme cold (Abaimov, 2010; Gower & Richards, 1990). In contrast, *P. sibirica* and *P. obovata* are shade-tolerant and meso-hygrophyte species (Chytrý et al., 2008; Tchebakova et al., 2016; Vaganov et al., 2006), growing under the canopy of other conifers and requiring moderate moisture availability. *P. sibirica* may reach high elevations in the Altai (Kharuk et al., 2017), whereas *P. obovata* competes with *L. sibirica* at its upper altitudinal limit and thrives with limited moisture availability (Holtmeier, 2009). All three species are adapted to cold environments (Hughes et al., 2019; Shah et al., 2020). Dendrochronological research in the Altai has predominantly focused on *L. sibirica* due to its strong climate sensitivity (Büntgen et al., 2016; Chen et al., 2012; Kirdyanov et al., 2024a; Tchebakova et al., 2016,), but *P. sibirica* has received less attention and *P. obovata* has been largely overlooked due to its lower sensitivity to climate fluctuations (Chytrý et al., 2008; Tchebakova et al., 2016).

Here, we assess the climate response of three co-occurring conifers species (i.e., *L. sibirica*, *P. sibirica* and *P. obovata*) in the Altai high mountain taiga by comparing their tree-ring width (TRW), latewood blue intensity (LWBI) and delta blue intensity (DBI) measurements against temperature and precipitation over the 1951–2021 period. In this study, we aim to determine whether LWBI and DBI enhance climate signal strength compared to TRW and to evaluate species-specific differences in climate sensitivity to ultimately improve temperature reconstructions in the area.

2. Materials and methods

2.1. Sampling design and study area

A total of 60 co-dominant trees (20 each of *L. sibirica*, *P. sibirica* and *P. obovata*) were sampled in a high mountain taiga mixed forest at 1620 m a.s.l. on a gentle southwest-facing slope near the Seminsky Pass (51°01’ N, 85°42' E; Fig. 1a) during the summer of 2022. One 5 mm increment core was collected from each tree at breast height (dbh). The tree sizes within the stand varied between the species, ranging in height from 17.7±3.5 m (mean±SD) in *P. sibirica* to 22.7±2.5 m in *L. sibirica*, while dbh from 33.7±6.6 cm in *P. obovata* to 56.1±10.5 cm in *L. sibirica* (Table S1).

The study area overlaps with the upper distribution limit of *P. obovata* around 1600 m a.s.l. (Bocharov, 2009; Ogureeva, 1980). From a phytogeographical perspective, this region falls within the central Altai mountainous zone, characterized by abundant coniferous forests. The upper forest limit spans an elevational range from 2100–2150 m a.s.l., predominantly consisting of open pine forests (Bocharov et al., 2002; Ogureeva, 1980). At the treeline of the Seminsky Pass, the upper mixed forest consists of pine, spruce, and larch species. Below this elevation, these mixed formations gradually transition into pure larch forests (Bocharov et al., 2002). Mountain-forest brown soils prevail within the upper forest limit, whereas mountain-forest chernozem soils are found below 1600-meter elevation (Davydov, 2003).

Meteorological data obtained from the nearby Onguday weather station (51° 24' N, 85° 36' E, 1700 m a.s.l.), located within 9 km of the sampling site, recorded a mean annual temperature of 0.35 ºC and annual precipitation totals of 374 mm for the 1951–2021 period (Fig. 1b). July registers as the warmest month at 16.9 ºC, while January stands as the coldest at -19.9 ºC.

Approximately 66% of the annual precipitation occurs between May and August (around 247 mm). Over the period since 1951, there has been a significant ($p < 0.01$) increase in mean annual and mean May-July temperatures of 0.31 ºC and 0.17 ºC per decade (Fig. 1c), respectively. However, non-significant trends in precipitation have been observed.

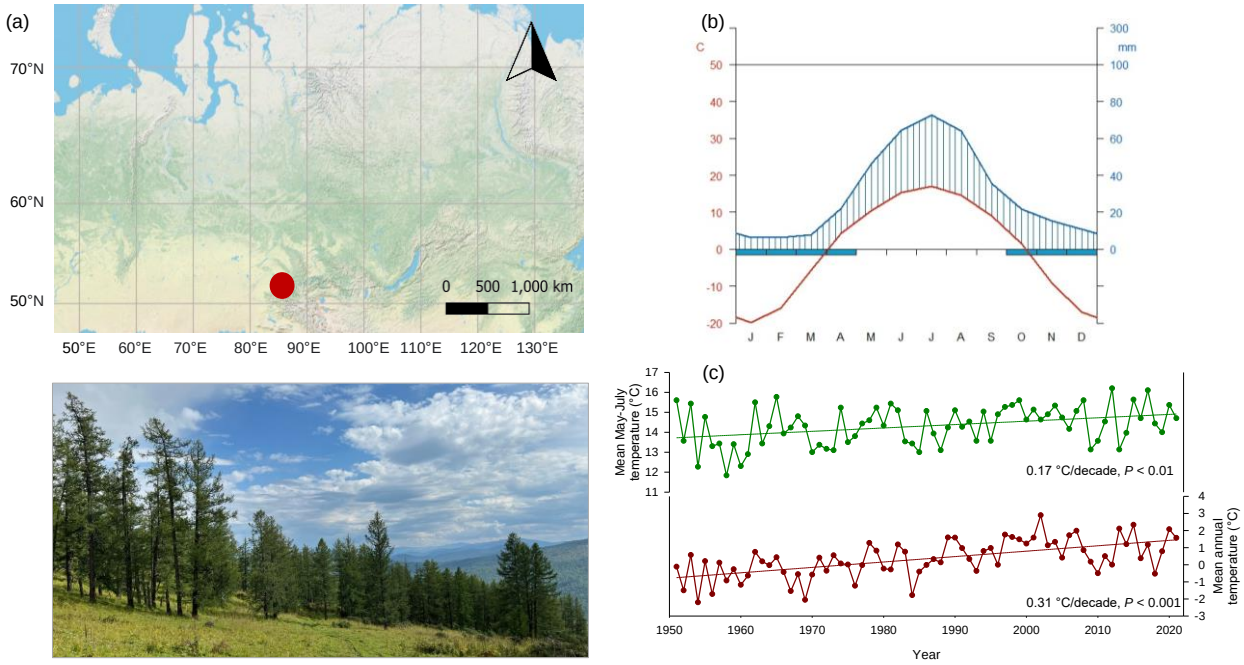

Figure 1. Location (red circle) and picture of the study site (a), climate diagram for the nearest station (Onguday) for the 1951–2021 period (b), and May-July and annual temperatures trends for the 1951–2021 period (c).

2.2. Tree-ring parameters and blue intensity measurements

Resin was extracted from the wood using ethanol (96%) in a Soxhlet apparatus for 72 hours, followed by the removal of water-soluble substances in warm water (80 °C) over 48 hours (Cerrato et al., 2023). Subsequently, the cores were airdried, fixed into wooden holders, and polished with progressively finer sandpaper up to 1200 grit size. Polished cores were scanned at 3200 dpi resolution using an Epson Perfection V800 flatbed scanner (Epson, Japan), calibrated with an IT8 Calibration Target color card (Fuji), and interfaced with Silverfast SE software

(LaserSoft Imaging, USA). The scanner was enclosed within a dark box during the scanning process to minimize the influence of external light sources on the final image (Agapova et al., 2024).

Tree-ring width (TRW), earlywood (EWW) and (LWW) latewood widths and earlywood (EWBI) and latewood blue intensity (LWBI) were measured on the digitized cores with CooRecoder version 9.3 (Cybis Elektronik & Data AB, Sweden). The software automatically calculated delta blue intensity (DBI) by subtracting EWBI from LWBI (Björklund et al., 2014). The obtained TRW series were visually cross-dated and cross-dating accuracy was verified using COFECHA (Holmes, 1983). Spline functions were fitted to the individual raw TRW, EWW, LWW, EWBI, LWBI and DBI measurement series with a 50% frequency cutoff at 32 years using the "dplR" package (Bunn, 2008) in the R environment (R Developmental Core Team, 2022), obtaining standardized series of high-frequency interannual variability (Cook and Peters, 1981). The standardized TRW, EWW, LWW, EWBI, LWBI and DBI series were further subject to autoregressive modeling to remove autocorrelation, producing residual chronologies (Cook and Kairiukstis, 1990). Bi-weight robust means of the residual versions of the standardized TRW measured series were used to produce residual index chronologies. Additionally, a linear regression between the EWW and LWW residual chronologies was applied to remove the dependence of LWW on EWW, obtaining an adjusted latewood (LWWadj) (Meko and Baisan, 2001). Finally, the robustness of the obtained mean chronologies was assessed via the expressed population signal (EPS), mean sensitivity (msx), mean inter-series correlation (R_{bt}), and signal-to-noise ratio (SNR).

2.3. Tree-ring and blue intensity parameters response to climate

Pearson's correlations were used to assess the climate sensitivity of each parameter-specific chronology for all species over the period 1951–2021. TRW, EWW, LWWadj, LWBI and DBI standard chronologies were correlated against monthly temperature means and precipitation totals. In addition, residual chronologies for the same parameters were correlated against detrended climate data, as suggested by Ols et al. (2023). All correlations were performed from September of the previous year to the current year September. To evaluate the cumulative effect of climate, we assessed the impact of May–July climate conditions, the period exhibiting the strongest climate signals. In addition, the Standardized Precipitation-Evapotranspiration Index (SPEI; Vicente-Serrano et al., 2010) was used to assess the effect of soil moisture availability on TRW, LWBI and DBI (1 to 6 months). Correlations were calculated for each time series from September of the previous year to September of the growth year over.

To assess the temporal stability of climate sensitivity, we selected the parameters showing the highest climate signals in monthly climate correlations (TRW, LWBI, and DBI standard chronologies). These were correlated against May, June, July, and May–July temperature means and precipitation totals, which were identified as the most important seasonal windows for tree growth among the studied species. Thirty-year moving correlations lagged by one year were calculated over the 1951–2021 period in the "Treeclim" R package (Zang and Biondi, 2015). Additionally, to evaluate the geographical predictive strength of TRW, LWBI and DBI standard chronologies, spatial field correlations against May-July temperature means were generated using the KNMI Climate Explorer (https://climexp.knmi.nl), based on the CRU TS 4.07 land temperature datasets (grid resolution of 0.5°).

2.4. Summer temperature reconstruction potential of LWBI and DBI among species

To assess the potential use of LWBI and DBI chronologies for summer temperature reconstruction in the region, regression models were developed using the "Treeclim" package in R, over the 1951–2021 period. Temperature reconstructions were calibrated using instrumental May–July temperature data for the period 1987–2021, while model validation was conducted across all three species for the 1951–1986 period. The accuracy of the reconstructions was evaluated using multiple statistical metrics, including Pearson's correlation coefficient (r), variance explained (R^2), adjusted explained variance (R^2 Adj), F-value, root-mean-square error (RMSE) reduction of error (RE) and coefficient of efficiency (CE).

3. Results

3.1. Tree growth and blue intensity measurements

Successful cross-dating was achieved for 58 trees, including 20 *P. sibirica* and *P. obovata*, alongside 18 *L. sibirica* trees (Table 1). However, for one *L. sibirica* sample, wood discoloration prevents obtaining BI data. The length of the tree-ring chronologies varies by species, ranging from 100 years (1922–2021) for *P. sibirica* and *P. obovata* to 261 years (1764–2021) for *L. sibirica* (chronologies for the common period 1951–2021 are shown in Fig. S1). Mean sensitivity, mean inter-series correlation, and signal-to-noise ratio range from 0.15 to 0.25, 0.21 to 0.50 and 5.4 to 17.8, respectively for the TRW chronologies, with *P. obovata* showing the lowest values and *L. sibirica* the highest. BI- derived chronologies range from 0.04 to 0.15, 0.23 to 0.30 and 5.55 to 8.02, respectively. EPS exceeds 0.85 for all the chronologies, with the highest values for *L. sibirica* TRW and EWW chronologies. However, exceptions are observed for *P. sibirica* EWW and LWWadj *P. obovata* LWWadj and.

Table 1. Characteristics of the tree-ring width (TRW), earlywood width (EWW), adjusted latewood (LWWadj), blue intensity (LWBI) and delta blue intensity (DBI) chronologies and their statistics for the 1951–2021 period.

Species	Parameter	No. trees	sl	ms_x	r_{bt}	SNR	EPS
Larix sibirica	TRW	18	261	0.25	0.50	17.80	0.95
	EWW	18	261	0.28	0.52	19.22	0.95
	LWWadj	18	261	0.33	0.37	10.34	0.91
	LWBI	17	261	0.04	0.30	7.27	0.88
	DBI	17	258	0.10	0.25	5.55	0.85
Pinus sibirica	TRW	20	100	0.16	0.27	7.26	0.88
	EWW	20	100	0.22	0.20	4.40	0.82
	LWWadj	20	100	0.50	0.07	1.48	0.60
	LWBI	20	100	0.06	0.24	6.41	0.87
	DBI	20	100	0.15	0.23	5.98	0.88
Picea obovata	TRW	20	100	0.15	0.21	5.42	0.85
	EWW	20	100	0.17	0.20	4.99	0.85
	LWWadj	20	100	0.29	0.15	3.56	0.78
	LWBI	20	100	0.05	0.29	8.02	0.89
	DBI	20	100	0.11	0.29	7.97	0.89

sl, series length; ms_x, mean sensitivity; r_{bt}, mean inter-series correlation; SNR, signal-to-noise ratio; EPS, expressed population signal.

3.2. Tree-ring and blue intensity parameters response to climate

The response of parameter-specific standard and residual chronologies is similar in timing and magnitude. Therefore, only the results for standard chronologies are shown (refer to Fig. S2 and Tables S2 and S3 for climate response of residual chronologies).

Summer temperatures positively affect TRW in all the species, though with species-specific differences in timing and intensity (Fig. 2). While *L. sibirica* and *P. obovata* show earlier signals in June ($r = 0.26$; $p < 0.05$ for both), *P. sibirica* peaks in July ($r = 0.33$; $p < 0.001$). The cumulative effect of mean May-July temperatures shows a higher correlation for *L. sibirica* ($r = 0.30$; $p < 0.01$) compared to the other two species. LWBI and DBI chronologies show stronger

and longer responses to mean monthly temperatures than TRW, particularly during May-July. *P. obovata* shows the highest LWBI signal in May and May-July temperatures (r = 0.57 and r = 0.70; $p < 0.001$, respectively). Similarly, *P. obovata* also shows the highest DBI signal in response to July and May-July temperatures (r = 0.56 and r = 0.70; $p < 0.001$, respectively). *L. sibirica* maximal LWBI and DBI responses to temperature occur during May-July (r = 0.44 and r = 0.47; $p < 0.001$, respectively), while *P. sibirica* maximal LWBI and DBI responses in July (r = 0.54 and $r = 0.49$; $p < 0.001$, respectively). EWW mimics TRW response in all the species, whereas *L. sibirica* LWWadj responds negatively to April temperatures (r = -0.44; $p < 0.001$) showing marginal positive responses to summer temperatures for all the species. EWBI shows earlier but weaker responses than LWBI and DBI, in April for *P. sibirica* and *P. obovata*, with maximal signals in May for all the species (Fig. S3).

Correlations with total monthly precipitation are generally weak and marginally significant (Fig. 2). TRW shows marginal positive correlations to previous December precipitation in *P. sibirica* (r = 0.24; $p < 0.05$) and current July precipitation in *L. sibirica* (r = 0.23; $P < 0.05$). Previous October correlates negatively with *P. obovata* (r = -0.28 $p < 0.01$). LWBI and DBI chronologies are negatively correlated with the current year summer precipitation. *P. obovata* shows the strongest LWBI and DBI responses to May-July precipitation (r = -0.35; $p < 0.01$ for both parameters). *L. sibirica* maximal LWBI and DBI responses occur in May (r = -0.29 and r = -0.33; $p < 0.01$, respectively), while *P. sibirica* maximal LWBI and DBI response occur in May-July (r = -0.28 and r = -0.30; $p < 0.01$ respectively). EWW mimics TRW precipitation response, whereas LWWadj and EWBI show minimal sensitivity to precipitation variability (Fig. S3). TRW, LWBI and DBI show negative correlations with SPEI suggesting a negative effect of wetter conditions in all the traits except *P. sibirica* TRW, which shows a significant positive response to previous November SPEI (Fig. S4).

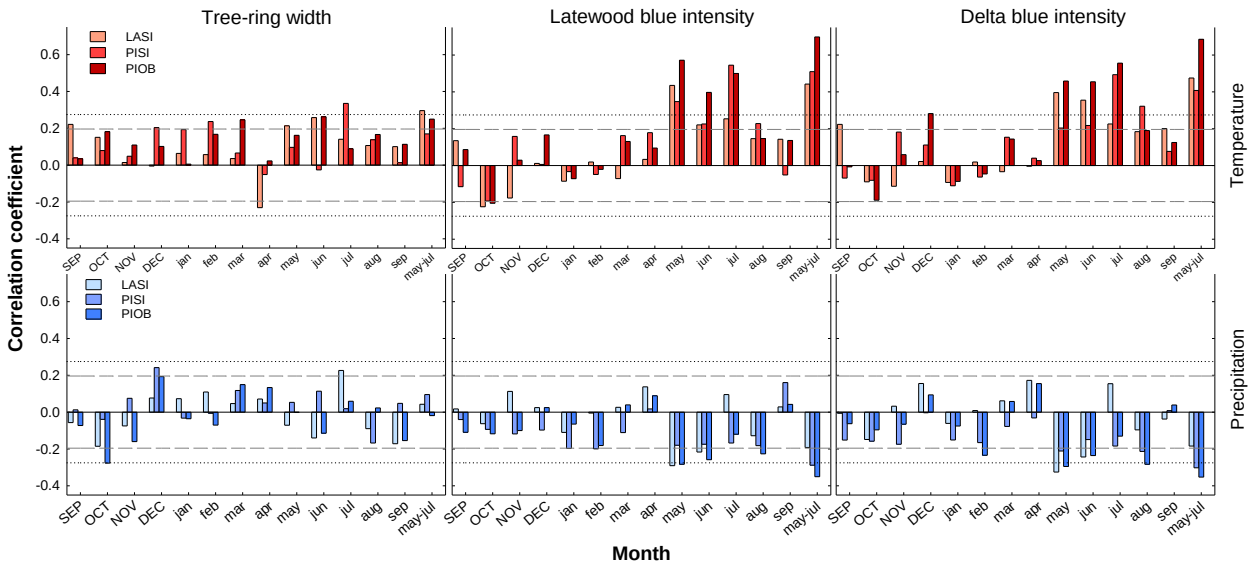

253

254 **Figure 2.** Pearson's correlation coefficients for tree-ring width, latewood blue intensity and delta
255 blue intensity standard chronologies with mean monthly temperature and total monthly
256 precipitation. Correlations were calculated for the growing season period, from previous year
257 September to current year September (including the aggregated May-July effect) over the 1951–
258 2021 period. Dashed and dotted lines represent significant correlation at $p < 0.05$ and $p < 0.01$,
259 respectively. LASI, *Larix sibirica*; PISI, *Pinus sibirica*; PIOB, *Picea obovata*.

260

261 *3.3. Temporal and spatial stability of climatic signals*

262

263 Thirty-year moving correlations against May, June, July, and May-July temperatures over the
264 1951–2021 period reveal high temporal instability across all the species and parameters.
265 However, *P. obovata* LWBI and DBI response to May-July temperatures remain stable and
266 highly significant throughout the period (Fig. 3). TRW response experiences fluctuations in all
267 the species and months, showing a general decreasing trend starting in the 1990's. LWBI
268 generally show higher stability than TRW, although differences between species arise. *L. sibirica*
269 response to May and June temperatures decrease and becomes non-significant, diverging from
270 the other two species which show a significant positive response. The response to July
271 temperature shows greater synchronicity between the species, with a breakpoint in the decreasing

trend during the 1990's. When considering the cumulative effect of May-July temperatures, *P. obovata* response remains notably stable, whereas *L. sibirica* and *P. sibirica* show asymmetric responses between each other. DBI mimics LWBI responses, with the response to May, July and May-July temperatures not differing much from LWBI, and a small difference in the response to June temperature between the species. *P. obovata* response to May-July temperatures remains stable during the studied period, although with a weak decline in the 2000's.

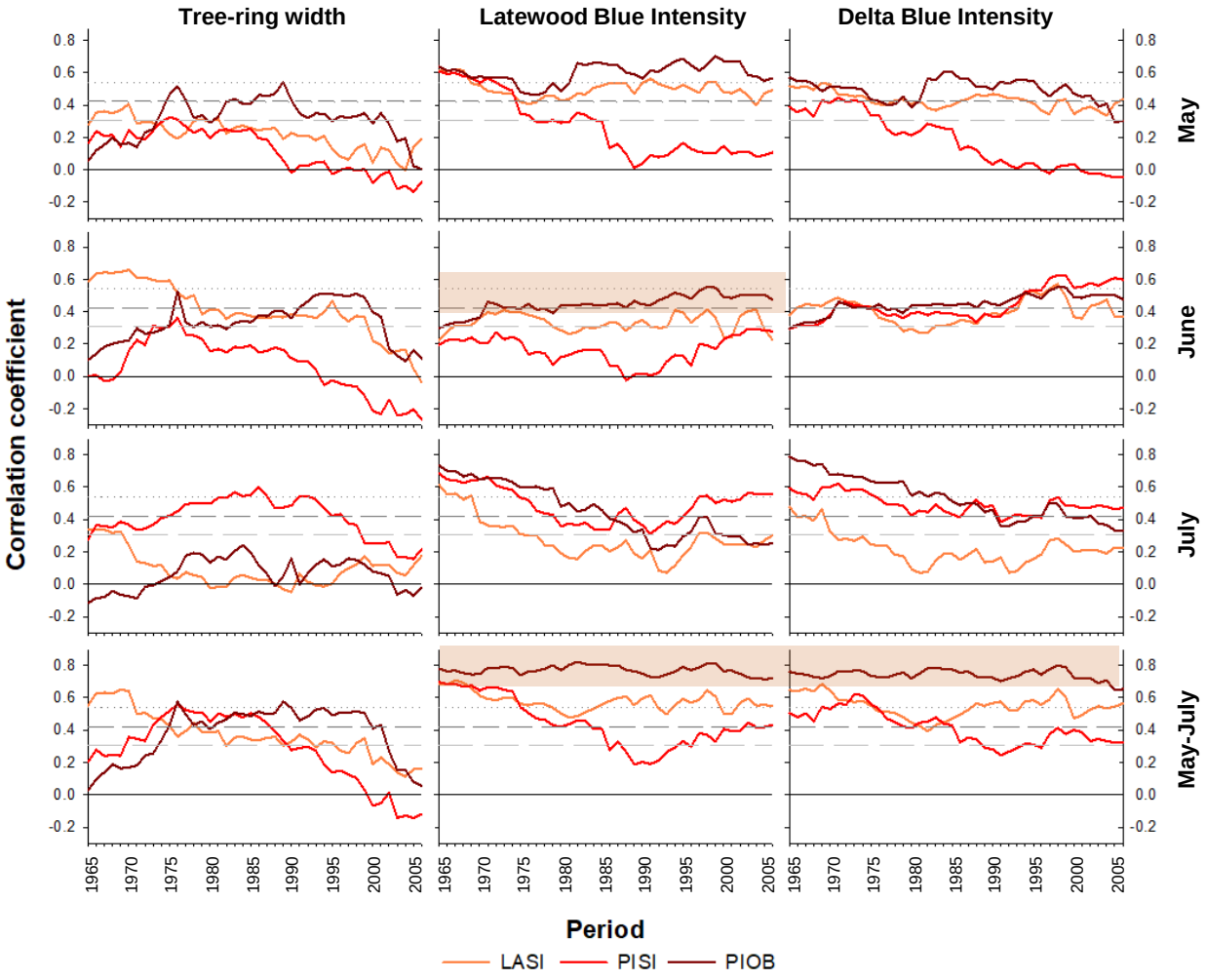

Figure 3. Thirty-year window moving correlations (1-year step) between tree-ring width, latewood blue intensity and delta blue intensity standard chronologies against May, June, July and May-July temperatures over the 1951–2021 period. The colored areas highlight the chronologies showing the higher temporal stability. Long dashed, medium dashed and dotted

horizonal lines represent significant correlation at $p < 0.05$ and $p < 0.01$ and $p < 0.001$, respectively. LASI, *Larix sibirica*; PISI, *Pinus sibirica*; PIOB, *Picea obovata*.

Spatial field correlations between TRW, LWBI and DBI chronologies against the cumulative effect of May-July mean temperatures over the 1951–2020 period reiterate the strong influence of summer temperatures on LWBI and DBI, as compared to TRW (Fig. 4). This influence is prominently pronounced in *P. obovata*. Besides showing strong responses, LWBI and DBI display an extensive geographic reach.

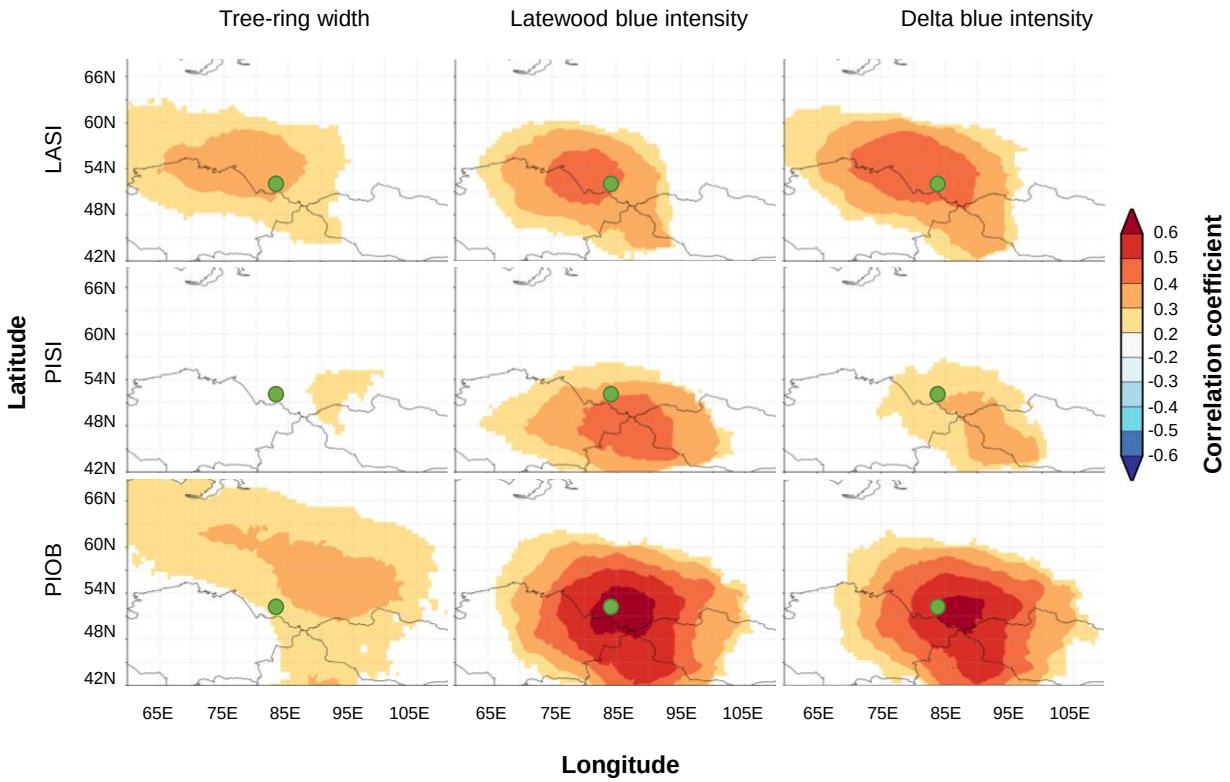

Figure 4. Spatial field correlations between tree-ring width, latewood blue intensity and delta blue intensity standard chronologies and May-July mean temperatures (CRU TS 4.06, 0.5º) over the 1951–2020 period. Green points represent the location of the sampling site. LASI, *Larix sibirica*; PISI, *Pinus sibirica*; PIOB, *Picea obovata*.

TRW, LWBI and DBI responses to precipitation remain mostly non-significant during the studied period, except for some exceptions (Fig. S5). *L. sibirica* TRW response to July precipitation reaches significant positive values from 1995. And although there is a clear sensitivity increase to July precipitations for all the parameters and species, only *L. sibirica* LWBI and DBI reaches marginal significant values in the 2000's.

3.4. Potential use of blue intensity parameters for temperature reconstruction

Regression models for May-July temperature reconstruction based on LWBI and DBI standard chronologies significantly correlate ($p < 0.05$) with mean May-July instrumental records for all the species (Table S4). However, *P. obovata* shows the highest coefficients during the calibration (1987–2021) and verification (1951–1986) periods for both parameters (Fig. 5). Correlations are stronger during the verification period. LWBI reaches r = 0.70 and 0.77 ($p < 0.001$) for calibration and verification, respectively, and DBI r = 0.65 and 0.75 ($p < 0.001$), respectively. In contrast, *P. sibirica* shows the lowest correlations during the calibration period, with LWBI (r = 0.36, $p < 0.05$) and DBI (r = 0.31, $p < 0.05$). During the verification period, the weakest correlations correspond to *L. sibirica* LWBI (r = 0.60, $p < 0.001$) and *P. sibirica* DBI (r = 0.53, $p < 0.001$). Regression models based on tree-ring width (TRW) chronologies do not show significant correlations with mean May–July temperatures, except for *L. sibirica* during the verification period (r = 0.53, $p < 0.001$; RMSE = 1.15; Table S4).

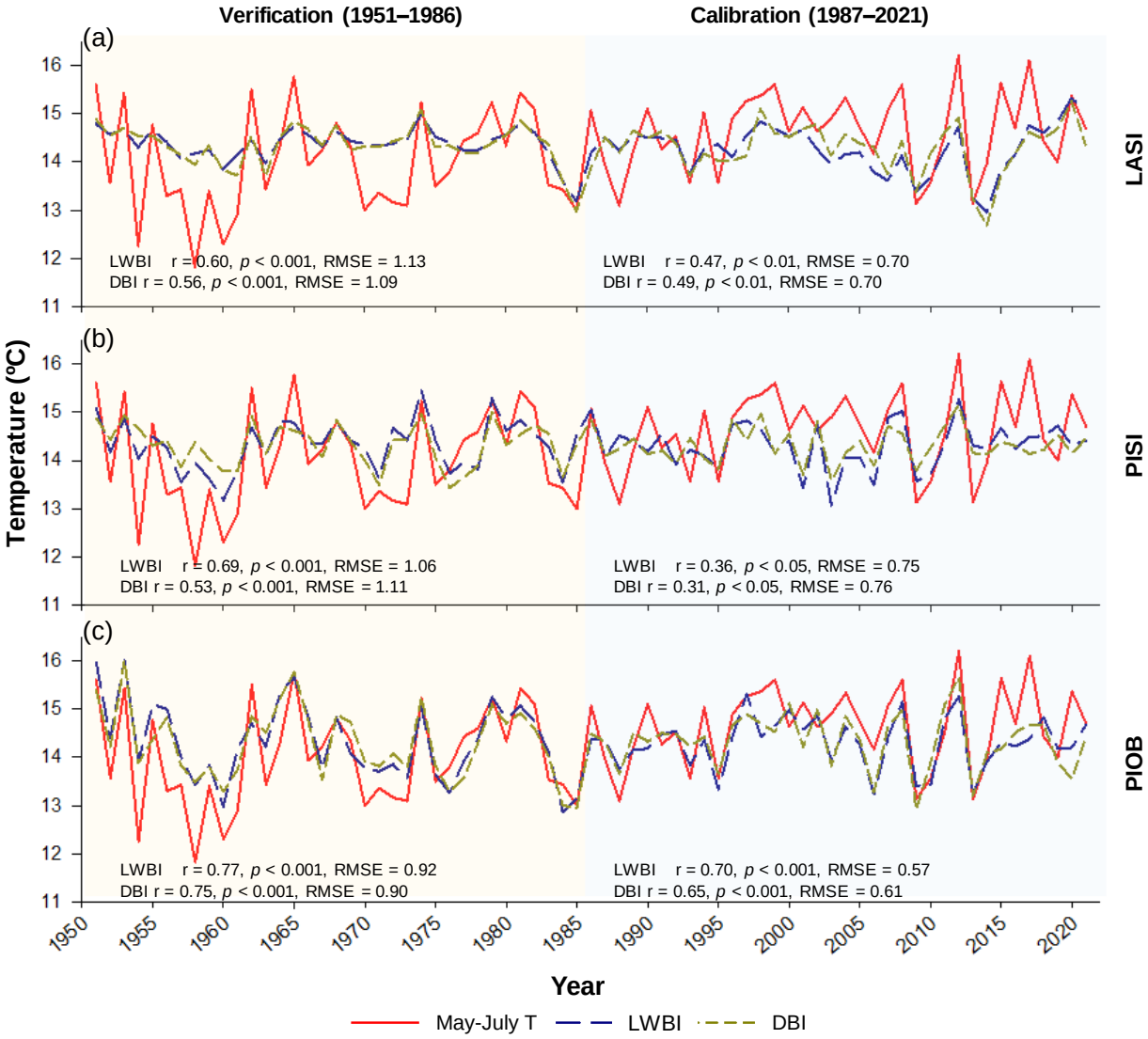

Figure 5. Regression models for May-July temperature reconstruction based on latewood blue intensity and delta blue intensity chronologies series over the 1951–2021 period (calibration: 1987–2021; verification: 1951–1986). Correlation coefficient against the mean May-July temperature, its significance and the root-mean-square error (RMSE) are shown for each period and species. (a) LASI, *Larix sibirica*; PISI, *Pinus sibirica*; PIOB, *Picea obovata.*

4. Discussion

The results reveal distinct species-specific responses of tree growth and blue intensity-derived parameters among the three studied conifer in the Altai high mountain taiga mixed. All species

respond positively to summer temperatures, but notable differences exist in the timing and magnitude of these climate signals. Additionally, LWBI and DBI show stronger and more temporal stable temperature signals than TRW, highlighting their potential as proxies for summer temperature.

L. sibirica is known as highly temperature-sensitive species (e.g., Kirdyanov et al., 2024a); however, our results do not highlight a particular higher sensitivity of this deciduous conifer comparted to the evergreen within the study area. Consistent with previous studies, *L. sibirica* radial growth (TRW) shows earlier sensitivity to late spring (May) and early summer (June) temperatures (Agapova et al., 2024; Bocharov, 2009; Chen et al., 2012; Hughes et al., 2019; Kirdyanov et al., 2024a, 2024b; Sidorova et al., 2012; Tainik et al., 2015; Zhou et al., 2021). The earlier response of *L. sibirica* TRW reflects a sooner onset of cambial activity and wood formation. An adaptation to thrive under extreme low temperatures allows this species it to maximize resource uptake at the onset of the growing season. In contrast, *P. sibirica* and *P. obovata* respond one month later (June and July, respectively), than in previous observations in the Altai, (May and June; Bocharov, 2009). Nevertheless, these results emphasize the relevance of temperature as a driving factor for tree radial growth at the beginning and during the growing season (Arzac et al., 2019; Kirdyanov et al., 2024c; Vaganov et al., 1999; Zhou et al., 2021).

The temperature signals in LWBI and DBI are stronger, occurring earlier and for longer than those in TRW, with *L. sibirica* and *P. obovata* responding in May and *P. sibirica* in June. *P. obovata* shows the strongest and longest seasonal temperature responses (from May to July). This contradicts the assumption that tree ring parameters of *P. obovata* are weaker climate proxies due to their lower sensitivity to temperature. The strong temperature dependence observed in the study area for *P. obovata* trees may be related to their location at the species' upper distribution limit. In contrast, *L. sibirica* and *P. sibirica*, which can grow beyond 2000 m

a.s.l. (Bocharov, 2009; Tainik et al., 2015), may be less constrained by temperature at this site. Consequently, *P. obovata*, growing near its upper limit, may benefit from rising temperatures, potentially alleviating its thermal constraints and promoting an upward shift in its range, ultimately altering the structure of the high mountain taiga in the region.

The moving correlations reveal temporal instability in temperature sensitivity. TRW shows a declining response since the 1990's. This pattern coincides with increasing summer temperatures in the region (Fig. S6), which may have reduced growth limitations in all three species. Despite co-occur under the same environmental conditions, changes in the significance of moving correlations for the three species are asynchronous. In contrast, LWBI and DBI in *P. obovata* maintain a relatively stable response to temperature, particularly in May–July, with only a slight weakening in the 2000s, likely due to recent warming. Our results indicate that *P. obovata* LWBI and DBI are promising proxies for reconstructing past May-July temperatures in the area, what is confirmed by strong correlations between the reconstruction and instrumental data. The strong temperature sensitivity observed in our study is comparable in strength to maximum latewood density (MXD; Agapova et al., 2024; Björklund et al., 2014; Heeter et al., 2021; Kirdyanov et al., 2024a; Wilson et al., 2014, 2017), a widely established proxy for summer temperature reconstructions in the Northern Hemisphere (e.g., Briffa et al., 2013; Davi, 2003; Esper et al., 2010; Grudd, 2008; Schneider et al., 2015). Although MXD has been extensively used, BI-derived parameters have received comparatively less attention. However, recent studies (e.g., Dolgova, 2016; Li and Li, 2023; Tsvetanov et al., 2020; Zheng and Wilson, 2024) have demonstrated their strong potential, supporting their application as viable alternatives to MXD.

The combination of positive temperature and negative precipitation signals across all species and parameters suggests that tree growth is not water-limited in the study area. This contrasts with water-limited environments such as the forest-steppe, where tree growth is strongly dependent on

precipitation (Arzac et al., 2021; Tabakova et al., 2020). Instead, the negative effects of precipitation on TRW and BI-derived parameters indicate that excess moisture may hinder tree growth, likely due to sufficient soil moisture from snowmelt earlier in the growing season (Bykov et al., 2023; Vaganov et al., 1999). Correlations with SPEI confirm than excessive water negatively influences radial growth and BI-derived parameters. These findings are consistent with previous studies in the region (Bocharov, 2009; Bykov et al., 2023) and suggest that moisture surpluses may restrict cambial activity. Moreover, moving correlations between precipitation and most of the parameters do not show significant signals, reinforcing the idea that water excess does not constrain tree growth in this environment. However, the increasing but still non-significant trend in sensitivity to July precipitations totals suggests that hydric balance in the area may be currently shifting, potentially leading to future water limitations under ongoing climate change.

Our results confirm species-specific responses to climate, as previously observed in mixed forests (e.g., Cao et al., 2019; Castagneri et al., 2014; Forrester et al., 2016; Kašpar et al., 2021). The response of these species is not solely determined by their physiological traits but is also influenced by ecological dynamics. Thus, species-specific responses are linked to site conditions, with the same species showing differential responses among sites (James, 2011; Kirdyanov et al., 2013; Zhou et al., 2021). Thus, *L. sibirica* likely established at the study site approximately 260 years ago, with open landscape conditions favoring its development as a pioneer and heliophytic species. As the canopy gradually closed and water availability became sufficient, the shade-tolerant and meso-hygrophytic species *P. sibirica* and *P. obovata* began to establish, around 100 years ago. A natural successional replacement of *L. sibirica* by other species, such as *P. sibirica*, would be expected, as previously observed in the Altai Mountains (Kharuk et al., 2010) and Mongolian forest patches (Li et al., 2019). Finally, the increasing incidence of wildfires in recent decades, linked to climate change (Ponomarev et al., 2016), may perturbate this succession

processes, by opening the forest canopy and, thus, favoring the initial succession stages dominated by *L. sibirica* (Day, 1972).

5. Conclusions

This study highlights the distinct species-specific responses of cohabiting coniferous species in the high mountain taiga mixed forest of the Russian Altai to climate variability, emphasizing the importance of considering individual species traits in climate impact assessments. The co-occurrence and succession dynamics of these conifer species suggest adaptive mechanisms to ongoing climate change, with warmer conditions favoring certain species and promoting upward shifts in their distribution limits, with significant implications for the future structure and composition of high mountain taiga forests. Our findings support LWBI and DBI as the most practical, temporally stable and geographically representative parameters to perform paleoclimatic reconstructions. Specifically, *P. obovata*, a commonly neglected species due to its low climate sensitivity, turned out to provide the most sensitive and robust climatic signal, which could be explained by the position of our sampling site at the altitudinal limit of the species distribution. Overall, we highlight the value of the blue intensity traits as long-term temperature proxies in the Altai Mountains and mid-latitude regions.

Acknowledgments

This work was carried out with the support of the Ministry of Science and Higher Education of the Russian Federation [FSRZ-2020-0014]. U.B. received fundings from the ERC Advanced Grant (# 882727; Monostar), and the ERC Synergy Grant (# 101118880; Synergy-Plague).

References

Abaimov, A.P., 2010. Geographical distribution and genetics of Siberian larch species. In Osawa, A., Zyryanova, O.A., Matssura, Y., Kajimoto, T., Wein, R.W. (eds). Permafrost Ecosystems Siberian Larch Forests. Springer

Agapova, V., Arzac, A., Kukarskih, V., Büntgen, U., Esper, J., Kirdyanov, A., 2024. Tree-ring Blue Intensity measurements from treeline sites in the Ural Mountains exhibit a strong summer temperature signal. Dendrochronologia. https://doi.org/10.1016/j.dendro.2024.126267

Arzac, A., Popkova, M., Anarbekova, A., Olano, J.M., Gutiérrez, E., Nikolaev, A., Shishov, V., 2019. Increasing radial and latewood growth rates of *Larix cajanderi* Mayr. and *Pinus sylvestris* L. in the continuous permafrost zone in Central Yakutia (Russia). Ann. For. Sci. 76. https://doi.org/10.1007/s13595-019-0881-4

Arzac, A., Tychkov, I., Rubtsov, A., Tabakova, M.A., Brezhnev, R., Koshurnikova, N., Knorre, A., Büntgen, U., 2021a. Phenological shifts compensate warming-induced drought stress in southern Siberian Scots pines. Eur. J. For. Res. 140, 1487–1498. https://doi.org/10.1007/s10342-021-01412-w

Barchenkov, A., Rubtsov, A., Safronova, I., Astapenko, S., Tabakova, K., Bogdanova, K., Anuev, E., Arzac, A., 2023. Features of Scots pine mortality due to incursion of pine bark beetles in symbiosis with ophiostomatoid fungi in the forest-steppe of Central Siberia. Forests 14 (7), 1301. https://doi.org/10.3390/f14071301

Barinov, V. V., Myglan, V.S., Nazarov, A.N., Vaganov, E.A., Agatova, A.R., Nepop, R.K., 2016. Extreme climatic events in the Altai Republic according to dendrochronological data. Biol. Bull. 43, 152–161. https://doi.org/10.1134/S1062359016020023

Bezuglova, N.N., Zinchenko, G.S., Malygina, N.S., Papina, T.S., Barlyaeva, T. V., 2012. Response of high-mountain Altai thermal regime to climate global warming of recent decades. Theor. Appl. Climatol. 110, 595–605. https://doi.org/10.1007/s00704-012-0710-2

461 Björklund, J.A., Gunnarson, B.E., Seftigen, K., Esper, J., Linderholm, H.W., 2014. Blue
462 intensity and density from northern fennoscandian tree rings, exploring the potential to
463 improve summer temperature reconstructions with earlywood information. Clim. Past 10,
464 877–885. https://doi.org/10.5194/cp-10-877-2014
465 Blyakharchuk, T.A., Wright, H.E., Borodavko, P.S., Van Der Knaap, W.O., Ammann, B., 2004.
466 Late Glacial and Holocene vegetational changes on the Ulagan high-mountain plateau, Altai
467 Mountains, southern Siberia. Palaeogeogr. Palaeoclimatol. Palaeoecol. 209, 259–279.
468 https://doi.org/10.1016/j.palaeo.2004.02.011
469 Bocharov, A., 2009. Climatogenetic radial growth of conifers in the upper forest belt of the
470 Seminsky Range (the Central Altai Mountains). J. Sib. Fed. Univ. Biol. 1, 30–37.
471 Bocharov, A., Vorobyeva, V., Ziganshin, R., 2002. Features of the inventory structure of cedar
472 stands along the altitudinal profile of the southern slope at the Seminsky Pass in the Central
473 Altai. Res. Nat. Taimyr.
474 Briffa, K.R., Melvin, T.M., Osborn, T., Hantemirov, R.M., Kirdyanov, A.V., Mazepa, V.S.,
475 Shiyatov, S.G., Esper, J., 2013. Reassessing the evidence for tree-growth and inferred
476 temperature change during the Common Era in Yamalia, northwest Siberia. Quat. Sci.
477 Rev. 72, 83–107. https://doi.org/10.1016/j.quascirev.2013.04.008
478 Bunn, A.G., 2008. A dendrochronology program library in R (dplR). Dendrochronologia 26,
479 115–124. https://doi.org/10.1016/j.dendro.2008.01.002
480 Büntgen, U., Myglan, V.S., Ljungqvist, F.C., McCormick, M., Di Cosmo, N., Sigl, M.,
481 Jungclaus, J., Wagner, S., Krusic, P.J., Esper, J., Kaplan, J.O., de Vaan, M.A.C.,
482 Luterbacher, J., Wacker, L., Tegel, W., Kirdyanov, A.V., 2016. Cooling and societal change
483 during the Late Antique Little Ice Age from 536 to around 660 AD. Nat. Geosci. 9, 231-
484 236. https://www.nature.com/articles/ngeo2652
485 Büntgen, U., Liebhold, A., Nievergelt, D., Wermelinger, B., Roques, A., Reinig, F., Krusic, P.J.,
486 Piermattei, A., Egli, S., Cherubini, P., Esper, J., 2020. Return of the moth: rethinking the

effect of climate on insect outbreaks. Oecologia 192, 543–552 . https://doi.org/10.1007/s00442-019-04585-9

Bykov, N.I., Shigimaga, A.A., Rygalova, N. V., 2023. Response of the radial growth of woody plants in the West Siberian Plain and adjacent mountainous territories to the characteristics of the snow cover. Forests 14. https://doi.org/10.3390/f14081690

Cao, J., Liu, H., Zhao, B., Li, Z., Drew, D.M., Zhao, X., 2019. Species-specific and elevation-differentiated responses of tree growth to rapid warming in a mixed forest lead to a continuous growth enhancement in semi-humid Northeast Asia. For. Ecol. Manage. 448, 76–84. https://doi.org/10.1016/j.foreco.2019.05.065

Castagneri, D., Nola, P., Motta, R., Carrer, M., 2014. Summer climate variability over the last 250years differently affected tree species radial growth in a mesic *Fagus-Abies-Picea* old-growth forest. For. Ecol. Manage. 320, 21–29. https://doi.org/10.1016/j.foreco.2014.02.023

Cazzolla Gatti, R., Callaghan, T., Velichevskaya, A., Dudko, A., Fabbio, L., Battipaglia, G., Liang, J., 2019. Accelerating upward treeline shift in the Altai Mountains under last-century climate change. Sci. Rep. 9, 1–13. https://doi.org/10.1038/s41598-019-44188-1

Cazzolla Gatti, R., Dudko, A., Lim, A., Velichevskaya, A.I., Lushchaeva, I. V., Pivovarova, A. V., Ventura, S., Lumini, E., Berruti, A., Volkov, I. V., 2018. The last 50 years of climate-induced melting of the Maliy Aktru glacier (Altai Mountains, Russia) revealed in a primary ecological succession. Ecol. Evol. 8, 7401–7420. https://doi.org/10.1002/ece3.4258

Cerrato, R., Salvatore, M.C., Carrer, M., Brunetti, M., Baroni, C., 2023. Blue intensity of Swiss stone pine as a high-frequency temperature proxy in the Alps. Eur. J. For. Res. 142, 933–948. https://doi.org/10.1007/s10342-023-01566-9

Chen, F., Yuan, Y.J., Wei, W.S., Fan, Z.A., Zhang, T.W., Shang, H.M., Zhang, R.B., Yu, S.L., Ji, C.R., Qin, L., 2012. Climatic response of ring width and maximum latewood density of *Larix sibirica* in the Altay Mountains, reveals recent warming trends. Ann. For. Sci. 69, 723–733. https://doi.org/10.1007/s13595-012-0187-2

513 Churakova (Sidorova), O.V., Myglan, V.S., Fonti, M.V., Naumova, O.V., Kirdyanov, A.V.,
514 Kalugin, I.A., Babich, V.V., Falster, G., Vaganov, E.A., Siegwolf, R.T.W., Saurer, M.,
515 2022. Modern aridity in the Altai-Sayan Mountain Range derived from multiple millennial
516 proxies. Sci. Rep. 12, 7752. https://doi.org/10.1038/s41598-022-11299-1
517 Chytrý, M., Danihelka, J., Kubešová, S., Lustyk, P., Ermakov, N., Hájek, M., Hájková, P., Kočí,
518 M., Otýpková, Z., Roleček, J., Řezníčková, M., Šmarda, P., Valachovič, M., Popov, D.,
519 Pišút, I., 2008. Diversity of forest vegetation across a strong gradient of climatic
520 continentality: Western Sayan Mountains, southern Siberia. Plant Ecol. 196, 61–83.
521 https://doi.org/10.1007/s11258-007-9335-4
522 Cook, E., Kairiukstis, L., 1990. Methods of dendrochronology – Applications in the
523 environmental sciences. Springer Netherlands, Dordrecht, Neatherlands.
524 Cook, E.R., Peters, K., 1981. The smoothing spline: a new approach to standardizing forest
525 interior tree-ring width series for dendroclimatic studies. Tree-ring Bull. 41, 45–53.
526 Davi, N.K., Jacoby, G.C., Wiles, G.C., 2003. Boreal temperature variability inferred from
527 maximum latewood density and tree-ring data, Wrangell Mountain region, Alaska.
528 Quaternary Research 60, 252–262. https://doi.org/10.1016/s0033-5894(03)00115-7
529 Davi, N.K., Rao, M.P., Wilson, R., Andreu-Hayles, L., Oelkers, R., D'Arrigo, R., Nachin, B.,
530 Buckley, B., Pederson, N., Leland, C., Suran, B., 2021. Accelerated recent warming and
531 temperature variability over the past eight centuries in the Central Asian Altai from blue
532 Intensity in Tree Rings. Geophys. Res. Lett. 48. https://doi.org/10.1029/2021GL092933
533 Davydov, V., 2003. Edaphic conditions for the growth of cedar forests in the subalpine and
534 sparse cedar belts of Altai. Cedar Probl.
535 Day, R.J., 1972. Stand structure, succession, and use of Southern Alberta ' s Rocky Mountain
536 Forest. Ecology 53, 472–478. https://doi.org/10.1002/abio.370040210

Dolgova, E., 2016. June–September temperature reconstruction in the Northern Caucasus based on blue intensity data. Dendrochronologia 39. http://dx.doi.org/10.1016/j.dendro.2016.03.002

Esper, J., Cook, E.R., Schweingruber, F.H., 2002. Low-frequency signals in long tree-ring chronologies for reconstructing past temperature variability. Science 295, 2250–2253. https://doi.org/10.1126/science.1066208

Esper. J., Büntgen, U., Frank, D.C., Nievergelt, D., Liebhold, A., 2007. 1200 years of regular outbreaks in alpine insects. Proc. R. Soc. B. 274671–679. http://doi.org/10.1098/rspb.2006.0191

Esper, J., Frank, D., Büntgen, U., Verstege, A., Hantemirov, R., Kirdyanov, A. V., 2010. Trends and uncertainties in Siberian indicators of 20th century warming. Glob. Chang. Biol. 16, 386–398. https://doi.org/10.1111/j.1365-2486.2009.01913.x

Esper, J., Schneider, L., Smerdon, J.E., Schöne, B.R., Büntgen, U., 2015. Signals and memory in tree-ring width and density data. Dendrochronologia 35, 62–70https://doi.org/10.1016/j.dendro.2015.07.001

Esper, J., Krusic, P. J., Ljungqvist, F. C., Luterbacher, J., Carrer, M., Cook, E., Davi, N. K., Hartl-Meier, C., Kirdyanov, A., Konter, O., Myglan, V., Timonen, M., Treydte, K., Trouet, V., Villalba, R., Yang, B., Büntgen, U., 2016. Ranking of tree-ring based temperature reconstructions of the past millennium. Quat. Sci. Rev.145, 134-151. https://doi.org/10.1016/j.quascirev.2016.05.009

Fonti, P., Bryukhanova, M. V., Myglan, V.S., Kirdyanov, A. V., Naumova, O. V., Vaganov, E.A., 2013. Temperature-induced responses of xylem structure of *Larix sibirica* (pinaceae) from the Russian Altay. Am. J. Bot. 100, 1332–1343. https://doi.org/10.3732/ajb.1200484

Forrester, D.I., Bonal, D., Dawud, S., Gessler, A., Granier, A., Pollastrini, M., Grossiord, C., 2016. Drought responses by individual tree species are not often correlated with tree species diversity in European forests. J. Appl. Ecol. 53, 1725–1734. https://doi.org/10.1111/1365-

563 2664.12745
564 Fritts, H.C. (1976) Tree Rings and Climate. Academic Press, London, 567 p.
565 Gower, S.T., Richards, J. H.,1990. Larches: deciduous conifers in an evergreen world.
566 BioScience, 40, 818–826. https://doi.org/10.2307/1311484
567 Grudd, H., 2008. Torneträsk tree-ring width and density AD 500-2004: a test of climatic
568 sensitivity and a new 1500-year reconstruction of north Fennoscandian summers. Clim.
569 Dyn. 31, 843–857. https://doi.org/10.1016/j.dendro.2018.02.002
570 Heeter, K.J., Harley, G.L., Maxwell, J.T., Wilson, R.J., Abatzoglou, J.T., Rayback, S.A.,
571 Rochner, M.L., Kitchens, K.A., 2021. Summer temperature variability since 1730 CE
572 across the low-to-mid latitudes of western North America from a tree ring blue intensity
573 network. Quat. Sci. Rev. 267, 107064. https://doi.org/10.1016/j.quascirev.2021.107064
574 Holmes, R.L., 1983. Computer-assisted quality control in tree-ring dating and measurement.
575 Tree-Ring Bulletin 43, 69-78.
576 Holtmeier, F.K., 2009. Mountain timberlines: Ecology, patchiness, and dynamics. Advanced
577 global change resource, Advances in Global Change Research.
578 Hughes, M.K., Olchev, A., Bunn, A.G., Berner, L.T., Losleben, M., Novenko, E., 2019.
579 Different climate responses of spruce and pine growth in Northern European Russia.
580 Dendrochronologia 56, 125601. https://doi.org/10.1016/j.dendro.2019.05.005
581 James, T.M., 2011a. Temperature sensitivity and recruitment dynamics of Siberian larch (*Larix*
582 *sibirica*) and Siberian spruce (*Picea obovata*) in northern Mongolia's boreal forest. For.
583 Ecol. Manage. 262, 629–636. https://doi.org/10.1016/j.foreco.2011.04.031
584 Jiang, S., Liang, H., Zhou, P., Wang, Z., Zhu, H., Kang, J., Huang, J.G., 2021. Spatial and
585 temporal differences in the response of *Larix sibirica* to climate change in the central Altai
586 Mountains. Dendrochronologia 67, 125827. https://doi.org/10.1016/j.dendro.2021.125827
587 Kang, J., Shishov, V. V., Tychkov, I., Zhou, P., Jiang, S., Ilyin, V.A., Ding, X., Huang, J.G.,
588 2022. Response of model-based cambium phenology and climatic factors to tree growth in

589 the Altai Mountains, Central Asia. Ecol. Indic. 143, 109393.
590 https://doi.org/10.1016/j.ecolind.2022.109393
591 Kašpar, J., Tumajer, J., Šamonil, P., Vašíčková, I., 2021. Species-specific climate-growth
592 interactions determine tree species dynamics in mixed Central European mountain forests.
593 Environ. Res. Lett. 16. https://doi.org/10.1088/1748-9326/abd8fb
594 Kharuk, V.I., Ranson, K.J., Dvinskaya, M.L., 2010. Evidence of evergreen conifers invasion into
595 larch dominated forests during recent decades. Adv. Glob. Chang. Res. 40, 53–65.
596 https://doi.org/10.1007/978-90-481-8641-9_4
597 Kharuk, V.I., Im, S.T., Dvinskaya, M.L., Ranson, K.J., Petrov, I.A., 2017. Tree wave migration
598 across an elevation gradient in the Altai Mountains, Siberia. J. Mt. Sci. 14, 442–452.
599 https://doi.org/10.1007/s11629-016-4286-7
600 Kirdyanov, A.V., Prokushkin, A.S., Tabakova, M.A., 2013. Tree-ring growth of Gmelin larch
601 under contrasting local conditions in the north of Central Siberia. Dendrochronologia 31,
602 114-119. https://doi.org/10.1016/j.dendro.2012.10.003
603 Kirdyanov, A.V., Arzac, A., kirdyanova, A.A., Arosio, T., Ovchinnikov, D.V., Ganyushkin,
604 D.A., Katjutin, P.N., Myglan, V.S., Nazarov, A.N., Slyusarenko, I.Y., Bebchuk, T.,
605 Büntgen, U, 2024a. Tree-ring chronologies from the upper treeline in the Russian Altai
606 Mountains reveal strong and stable summer temperature signals. Forests.
607 https://doi.org/10.3390/f15081402
608 Kirdyanov, A.V., Kolmogorov, A.I., Krus, S., Herzschuh, U., Arzac, A., Pestryakova, L.A.,
609 Nikolaev, A.N., Bebchuk, T., Büntgen, U., 2024b. Arctic amplification causes earlier onset
610 of seasonal tree growth in northeastern Siberia. Environ. Res. Lett. 19, 114091.
611 https://doi.org/10.1088/1748-9326/ad845f
612 Kirdyanov, A.V., Saurer, M., Arzac, A., Knorre, A.A., Prokushkin, A.S., Churakova (Sidorova),
613 O. V., Arosio, T., Bebchuk, T., Siegwolf, R., Büntgen, U., 2024c. Thawing permafrost can
614 mitigate warming-induced drought stress in boreal forest trees. Sci. Total Environ. 912.

https://doi.org/10.1016/j.scitotenv.2023.168858

Li, H., Kawada, K., Ohashi, H., Jamsran, U., Hu, X., Tamura, K., Kamijo, T., 2019. Regeneration of *Larix sibirica* boreal forest patches in the forest-steppe ecotone in Gorkhi Terelj National Park, Mongolia. J. For. Res. 24, 52–60. https://doi.org/10.1080/13416979.2018.1557101

Li, T., Li, J., 2032. August Temperature Reconstruction Based on Tree-Ring Latewood Blue Intensity in the Southeastern Tibetan Plateau. Forests 14(7). https://doi.org/10.3390/f14071441

Meko, D.M., Baisan, C.H., 2001. Pilot study of latewood-width of conifers as an indicator of variability of summer rainfall in the North American monsoonregion. Int. J. Climatol. 21, 697–708. https://doi.org/10.1002/joc.646

Mukhanova, M. V., Syromyatina, M. V., Chistyakov, K. V., 2016. Reconstructing the hydrometeorological indicators in the mountains of Southwestern Tuva and Northwestern Mongolia from dendrochronological data. Geogr. Nat. Resour. 37, 144–150. https://doi.org/10.1134/S1875372816020086

Myglan, V.S., Oidupaa, O.C., Kirdyanov, A.V., Vaganov, E.A., 2008. 1929-Year Tree-Ring Chronology for the Altai-Sayan Region (Western Tuva). Archaeol. Ethnol. Anthropol. Eurasia 4, 25–31. https://doi.org/10.1016/j.aeae.2009.03.003

Myglan, V., Barinov, V. V., Nazarov, A.N., 2015. A millennium-long tree-ring chronologies Koksu and Tara on Altay. J. Sib. Fed. Univ. Biol. 8, 319–332. https://doi.org/10.17516/1997-1389-2015-8-3-319-332

Myglan, V.S., Zharnikova, O.A., Malysheva, N. V., Gerasimova, O. V., Vaganov, E.A., Sidorova, O. V., 2012. Constructing the tree-ring chronology and reconstructing summertime air temperatures in southern Altai for the last 1500 years. Geogr. Nat. Resour. 33, 200–207. https://doi.org/10.1134/S1875372812030031

Ogureeva, G., 1980. Botanical Geography of Altai. Nauka, Moscow.

Ols, C., Klesse, S., Girardin, M.P., Evans, M.E.K., DeRose, R.J., Trouet, V., 2023. Detrending climate data prior to climate–growth analyses in dendroecology: A common best practice? Dendrochronologia 79. https://doi.org/10.1016/j.dendro.2023.126094

Ovtchinnikov, D., Adamenko, M., Panushkina, I., 2000. A 1105-year tree-ring chronology in Altai region and its application for reconstruction of summer temperatures. Geolines 11, 121–122.

Ponomarev, E.I., Kharuk, V.I., Ranson, K.J., 2016. Wildfires dynamics in Siberian larch forests. Forests 7, 1–9. https://doi.org/10.3390/f7060125

R Developmental Core Team, R., 2022. R: A Language and environment for statistical computing. URL. R Foundation for Statistical Computing, Vienna, Austria.

Schneider, L., Smerdon, J.E., Büntgen, U., Wilson, R.J.S., Myglan, V.S., Kirdyanov, A.V., Esper, J., 2015. Revising midlatitude summer temperatures back to A.D. 600 based on a wood density network. Geophys. Res. Lett. 42, 4556–4562. https://doi.org/10.1002/2015GL063956

Shah, S., Yu, J., Liu, Q., Shi, J., Ahmad, A., Khan, D., Mannan, A., 2020. Climate growth response of *Pinus sibirica* (Siberian pine) in the altai mountains, northwestern China. Pakistan J. Bot. 52, 593–600. https://doi.org/10.30848/PJB2020-2(16)

Shah, S., Yu, J., Liu, Q., Zhou, G., Yan, G., Zhou, H., Hussain, M., Hussain, A., Habiba, U., Khalid, F., Ullah, S., Rahim, F., Adil, M., Zeb, U., Ambrin, 2023. The Siberian pine growth dynamics in Altai Mountains, China. Brazilian J. Biol. 83. https://doi.org/10.1590/1519-6984.244011

Sidorova, O. V., Saurer, M., Myglan, V.S., Eichler, A., Schwikowski, M., Kirdyanov, A. V., Bryukhanova, M. V., Gerasimova, O. V., Kalugin, I.A., Daryin, A. V., Siegwolf, R.T.W., 2012. A multi-proxy approach for revealing recent climatic changes in the Russian Altai. Clim. Dyn. 38, 175–188. https://doi.org/10.1007/s00382-010-0989-6

Sidorova, O. V., Siegwolf, R.T.W., Myglan, V.S., Ovchinnikov, D. V., Shishov, V. V., Helle,

667 G., Loader, N.J., Saurer, M., 2013. The application of tree-rings and stable isotopes for
668 reconstructions of climate conditions in the Russian Altai. Clim. Change 120, 153–167.
669 https://doi.org/10.1007/s10584-013-0805-5
670 Tabakova, M.A., Arzac, A., Martínez, E., Kirdyanov, A. V., 2020. Climatic factors controlling
671 *Pinus sylvestris* radial growth along a transect of increasing continentality in southern
672 Siberia. Dendrochronologia 62. https://doi.org/10.1016/j.dendro.2020.125709
673 Tainik, A. V., Myglan, V.S., Barinov, V. V., Nazarov, A.N., Agatova, A.R., Nepop, R.K., 2015.
674 Tree-ring growth of Siberian larch at the upper treeline in the Altai Republic. Izv. Ross.
675 Akad. Nauk. Seriya Geogr. 61. https://doi.org/10.15356/0373-2444-2015-6-61-71
676 Tchebakova, N.M., Parfenova, E.I., Korets, M.A., Conard, S.G., 2016. Potential change in forest
677 types and stand heights in central Siberia in a warming climate. Environ. Res. Lett. 11.
678 https://doi.org/10.1088/1748-9326/11/3/035016
679 Tsvetanov, N., Dolgova, E., Panayotov, M., 2020. First measurements of Blue intensity from
680 *Pinus peuce* and *Pinus heldreichii* tree rings and potential for climate reconstructions.
681 Dendrochronologia 60. https://doi.org/10.1016/j.dendro.2020.125681
682 Vaganov, E.A., Hughes, M.K., Kirdyanov, A.V., Schweingruber, F.H., Silkin, P.P., 1999.
683 Influence of snowfall and melt timing on tree growth in subarctic Eurasia. Nature 400, 149–
684 151. https://doi.org/10.1038/22087
685 Vaganov, E. A., Hughes, M. K., & Shashkin, A. V., 2006. Growth dynamics of conifer tree
686 rings: images of past and future environments (Vol. 183). Springer Science & Business
687 Media.
688 Vicente-Serrano, S.M., Beguería, S., Lopez-Moreno, J.I., 2010. A multiscalar drought index
689 sensitive to global warming: the standardized precipitation evapotranspiration index. J.
690 Clim. 23, 1696–1718. https://doi.org/10.1175/2009JCLI2909.1
691 Wang, W., Huang, J.G., Zhang, T., Qin, L., Jiang, S., Zhou, P., Zhang, Y., Peñuelas, J., 2023.
692 Precipitation regulates the responses of xylem phenology of two dominant tree species to

693 temperature in arid and semi-arid forest of the southern Altai Mountains. Sci. Total
694 Environ. 886. https://doi.org/10.1016/j.scitotenv.2023.163951
695 Wilson, R., Rao, R., Rydval, M., Wood, C., Larsson, L.Å., Luckman, B.H., 2014. Blue Intensity
696 for dendroclimatology: The BC blues: A case study from British Columbia, Canada.
697 Holocene 24, 1428–1438. https://doi.org/10.1177/0959683614544051
698 Wilson, R., D'Arrigo, R., Andreu-Hayles, L., Oelkers, R., Wiles, G., Anchukaitis, K., Davi, N.,
699 2017. Experiments based on blue intensity for reconstructing North Pacific temperatures
700 along the Gulf of Alaska. Clim. Past 13, 1007–1022. https://doi.org/10.5194/cp-13-1007-
701 2017
702 Zang, C., Biondi, F., 2015. Treeclim: An R package for the numerical calibration of proxy-
703 climate relationships. Ecography (Cop.). 38, 431–436. https://doi.org/10.1111/ecog.01335
704 Zheng, Y., Wilson, R., 2024. Tree Ring Blue Intensity-Based August Temperature
705 Reconstruction for Subtropical Central China. Forests 15(8).
706 https://doi.org/10.3390/f15081428
707 Zhou, P., Huang, J.G., Liang, H., Rossi, S., Bergeron, Y., Shishov, V. V., Jiang, S., Kang, J.,
708 Zhu, H., Dong, Z., 2021. Radial growth of *Larix sibirica* was more sensitive to climate at
709 low than high altitudes in the Altai Mountains, China. Agric. For. Meteorol. 304–305,
710 108392. https://doi.org/10.1016/j.agrformet.2021.108392
711

712 **Supplements**

713

714 **Table S1.** Metrics of sampled trees per specie. LASI, *Larix sibirica*; PISI, *Pinus sibirica*; PIOB,

715 *Picea obovata*.

716

	Tree height (mean±SD)	Diameter at breast height (mean±SD)	Tree age (mean±SD)
LASI	22.7±2.5	56.1±10.5	162.5±71.3
PISI	17.7±1.7	49.2±10.1	88.5±13.3
PIOB	19.1±3.5	33.7±6.6	87.8±14.1

717

718

Table S2. Pearson's correlation coefficients for tree-ring width (TRW), latewood blue intensity (LWBI) and delta blue intensity (DBI) standard and residual chronologies with mean monthly temperature. Correlations were calculated for the growing season period, from previous year September to current year September (including the aggregated May-July effect) over the 1951–2021 period. LASI, *Larix sibirica*; PISI, *Pinus sibirica*; PIOB, *Picea obovata*.

	Month	TRW (standard)	TRW (residual)	LWBI (standard)	LWBI (residual)	DBI (standard)	DBI (residual)
LASI	SEP	*0.22*	–	–	–	*0.22*	–
	OCT	–	–	*-0.22*	*-0.23*	–	–
	NOV	–	–	–	–	–	–
	DEC	–	–	–	–	–	–
	jan	–	–	–	–	–	–
	feb	–	–	–	–	–	–
	mar	–	–	–	–	–	–
	apr	*-0.23*	-0.34	–	*0.20*	–	–
	may	*0.21*	–	**0.43**	**0.51**	**0.40**	**0.45**
	jun	*0.26*	0.32	*0.22*	0.32	0.35	**0.44**
	jul	–	*0.20*	*0.25*	**0.39**	*0.23*	0.32
	aug	–	–	–	*0.25*	–	0.30
	sep	–	–	–	–	*0.20*	–
	may-jul	0.30	0.35	**0.44**	**0.60**	**0.47**	**0.60**
PISI	SEP	–	–	–	–	–	–
	OCT	–	–	–	*-0.21*	–	–
	NOV	–	–	–	–	–	–
	DEC	*0.20*	–	–	–	–	–
	jan	–	*0.21*	–	–	–	–
	feb	*0.24*	–	–	–	–	–
	mar	–	–	–	–	–	*0.20*
	apr	–	–	–	*0.23*	–	–
	may	–	–	0.35	0.35	*0.20*	*0.20*
	jun	–	–	*0.23*	*0.23*	*0.22*	*0.25*
	jul	0.33	0.32	**0.54**	**0.58**	**0.49**	**0.54**
	aug	–	–	*0.23*	*0.23*	0.32	**0.38**
	sep	–	–	–	–	–	–
	may-jul	–	–	**0.51**	**0.54**	**0.41**	**0.45**
PIOB	SEP	–	–	–	–	–	–
	OCT	–	–	*-0.21*	*-0.24*	–	*-0.21*
	NOV	–	–	–	–	–	–
	DEC	–	–	–	–	0.28	0.31
	jan	–	–	–	–	–	–
	feb	–	–	–	–	–	–
	mar	*0.25*	–	–	–	–	–
	apr	–	–	–	–	–	–
	may	–	–	**0.57**	**0.59**	**0.46**	**0.48**
	jun	*0.26*	0.32	**0.40**	**0.43**	**0.45**	**0.48**
	jul	–	–	**0.50**	**0.58**	**0.56**	**0.61**
	aug	–	–	–	*0.20*	–	*0.23*
	sep	–	–	–	–	–	–
	may-jul	*0.25*	–	**0.70**	**0.78**	**0.69**	**0.75**

Only significant values are shown. Coefficients in bold are significant at p <0.001, underlined coefficients are significant at p <0.01 and coefficients in italic are significant at p <0.05.

Table S3. Pearson's correlation coefficients for tree-ring width (TRW), latewood blue intensity (LWBI) and delta blue intensity (DBI) standard and residual chronologies with mean total precipitation. Correlations were calculated for the growing season period, from previous year September to current year September (including the aggregated May-July effect) over the 1951–2021 period. LASI, *Larix sibirica*; PISI, *Pinus sibirica*; PIOB, *Picea obovata*.

	Month	TRW (standard)	TRW (residual)	LWBI (standard)	LWBI (residual)	DBI (standard)	DBI (residual)
LASI	SEP	–	–	–	–	–	–
	OCT	–	*-0.25*	–	–	–	–
	NOV	–	–	–	*0.24*	–	–
	DEC	–	–	–	–	–	–
	jan	–	–	–	*-0.22*	–	–
	feb	–	–	–	–	–	–
	mar	–	–	–	–	–	–
	apr	–	–	–	–	–	–
	may	–	–	-0.29	*-0.27*	-0.33	-0.30
	jun	–	–	*-0.22*	–	*-0.24*	*-0.22*
	jul	*0.23*	–	–	–	–	–
	aug	–	–	–	–	–	–
	sep	–	–	–	–	–	–
	may-jul	–	–	–	*-0.23*	–	*-0.21*
PISI	SEP	–	–	–	–	–	–
	OCT	–	–	–	–	–	–
	NOV	–	–	–	–	–	*-0.21*
	DEC	*0.24*	–	–	–	–	–
	jan	–	–	*-0.20*	*-0.22*	–	–
	feb	–	–	*-0.20*	*-0.20*	–	–
	mar	–	–	–	–	–	–
	apr	–	–	–	–	–	–
	may	–	–	–	–	*-0.21*	*-0.21*
	jun	–	–	–	–	–	–
	jul	–	–	–	–	–	–
	aug	–	–	–	–	*-0.21*	*-0.20*
	sep	–	–	–	–	–	–
	may-jul	–	–	-0.29	*-0.26*	-0.30	*-0.23*
PIOB	SEP	–	–	–	–	–	–
	OCT	-0.28	*-0.23*	–	–	–	–
	NOV	–	*-0.21*	–	–	–	–
	DEC	–	–	–	–	–	–
	jan	–	–	–	–	–	–
	feb	–	–	–	–	*-0.23*	*-0.22*
	mar	–	–	–	–	–	–
	apr	–	–	–	–	–	–
	may	–	–	-0.28	*-0.24*	-0.30	*-0.26*
	jun	–	*-0.23*	–	-0.30	*-0.24*	*-0.25*
	jul	–	–	–	–	–	–
	aug	–	–	*-0.23*	-0.30	-0.28	-0.31
	sep	–	–	–	–	–	–
	may-jul	–	–	-0.35	-0.34	-0.35	-0.32

Only significant values are shown. Coefficients in bold are significant at $p < 0.001$, underlined coefficients are significant at $p < 0.01$ and coefficients in italic are significant at $p < 0.05$.

Table S4. Statistics of May-July temperature reconstructions based on blue intensity (BI) and delta blue intensity (DBI) for the calibration (1987–2021) and verification (1951–1986) periods.

		Larix sibirica		*Pinus sibirica*		*Picea obovata*	
		LWBI	DBI	LWBI	DBI	LWBI	DBI
Calibration 1987 – 2021	r	0.47	0.49	0.36	0.31	0.70	0.65
	R^2	0.24	0.26	0.13	0.09	0.50	0.43
	R^2 Adj	0.22	0.23	0.10	0.06	0.49	0.41
	F-value	10.35	11.12	4.58	3.07	32.38	23.72
	RMSE	0.71	0.70	0.75	0.76	0.57	0.61
	RE	–	–	–	–	–	–
	CE	–	–	–	–	–	–
Verification 1951 – 1986	r	0.60	0.56	0.69	0.53	0.77	0.75
	R^2	0.33	0.29	0.45	0.25	0.56	0.54
	R^2 Adj	0.31	0.27	0.44	0.23	0.54	0.53
	F-value	16.26	13.39	27.30	11.08	41.36	38.73
	RMSE	1.13	1.10	1.06	1.11	0.92	0.90
	RE	0.11	0.16	0.22	0.15	0.41	0.44
	CE	-0.22	-0.15	-0.10	-0.17	0.19	0.23

r, Pearson's correlation coefficient; R^2, variance explained; R^2 Adj, adjusted explained variance; F-value, RMSE, root-mean-square error; RE, reduction of error; CE, coefficient of efficiency.

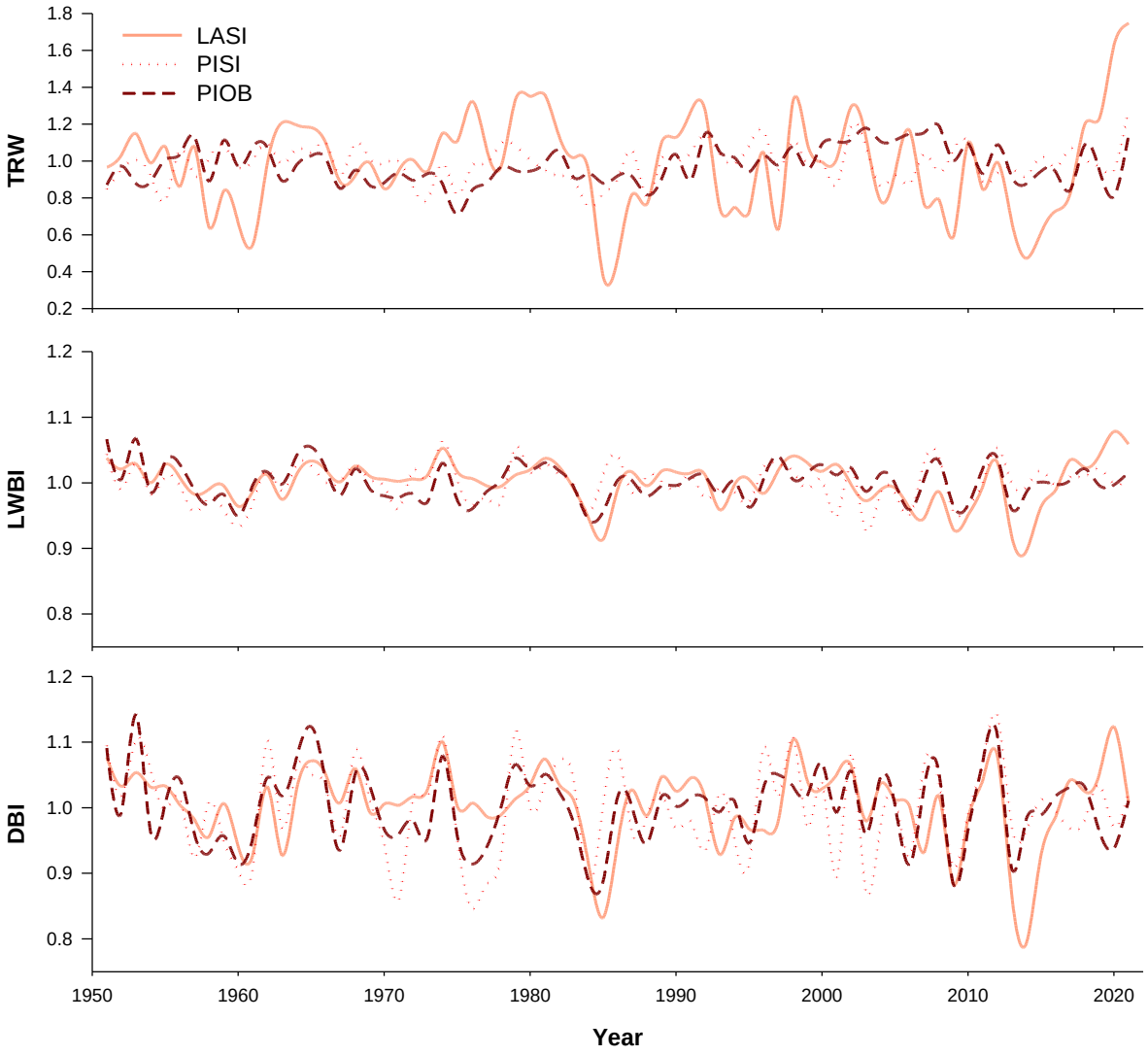

738

739 **Figure S1.** Tree-ring width (TRW), latewood blue intensity (LWBI) and delta blue intensity

740 (DBI) standard chronologies for the common 1951–2021 period. LASI, *Larix sibirica*; PISI,

741 *Pinus sibirica*; PIOB, *Picea obovata*.

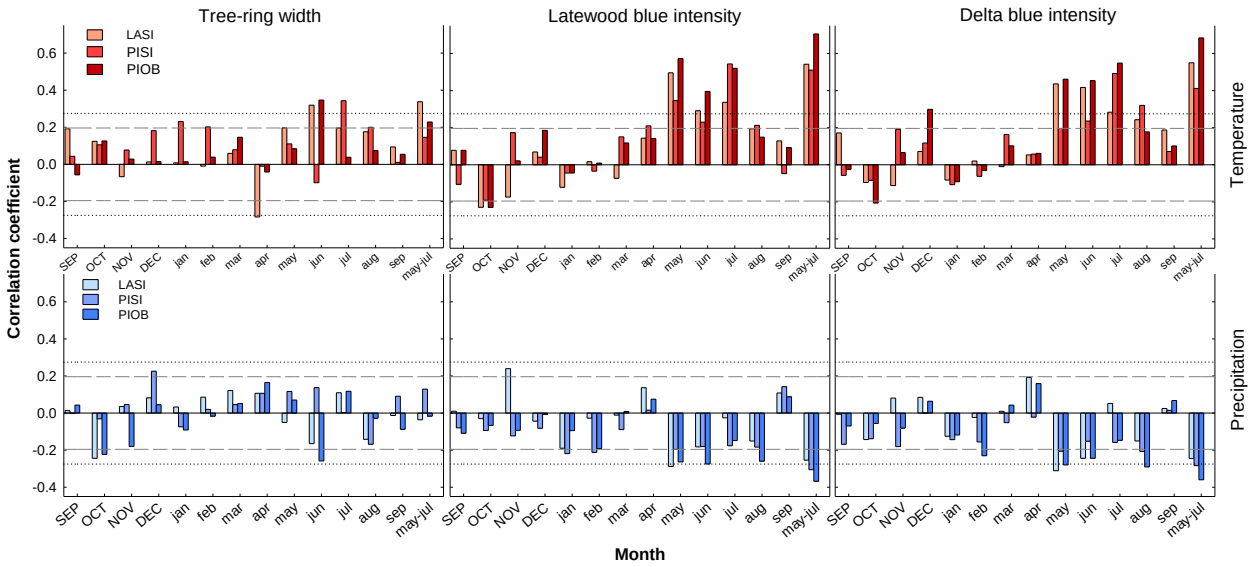

742

743 **Figure S2.** Pearson's correlation coefficients for tree-ring width, latewood blue intensity and

744 delta blue intensity residual chronologies with detrended mean monthly temperature and total

745 monthly precipitation. Correlations were calculated for the growing season period, from previous

746 year September to current year September (including the aggregated May-July effect) over the

747 1951–2021 period. Dashed and dotted lines represent significant correlation at $p < 0.05$ and $p <$

748 0.01, respectively. LASI, *Larix sibirica*; PISI, *Pinus sibirica*; PIOB, *Picea obovata*.

749

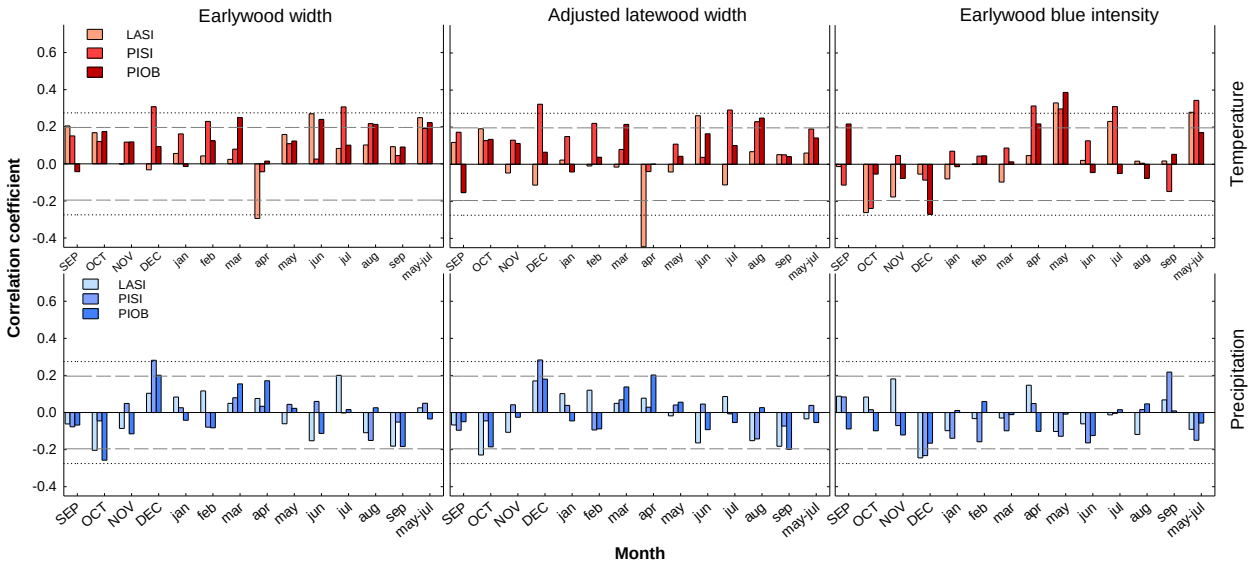

750

751 **Figure S3.** Pearson's correlation coefficients for earlywood width, adjusted latewood and

752 earlywood blue intensity standard chronologies with mean monthly temperature and total

monthly precipitation. Correlations were calculated for the growing season period, from previous year September to current year September (including the aggregated May-July effect) over the 1951–2021 period. Dashed and dotted lines represent significant correlation at $p < 0.05$ and $p < 0.01$, respectively. LASI, *Larix sibirica*; PISI, *Pinus sibirica*; PIOB, *Picea obovata*.

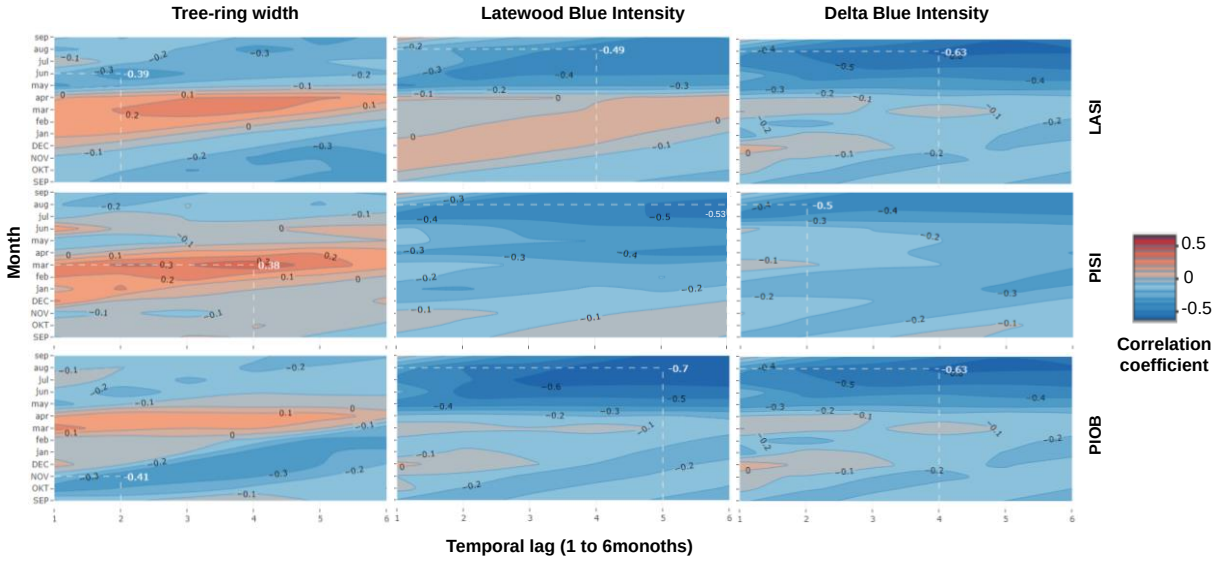

Figure S4. Pearson's correlations between tree-ring width, latewood blue intensity and delta blue intensity standard chronologies and monthly Standardized Precipitation–Evaporation index (SPEI) series at different time scales (1 to 6 months) for the 1951–2021 period. The correlations were calculated from September of the previous year (uppercase letters) to September of the current year (lowercase letters). Inserts in the plots represent the month and temporal lag in which maximum significant correlation coefficients occur. LASI, *Larix sibirica*; PISI, *Pinus sibirica*; PIOB, *Picea obovata*.

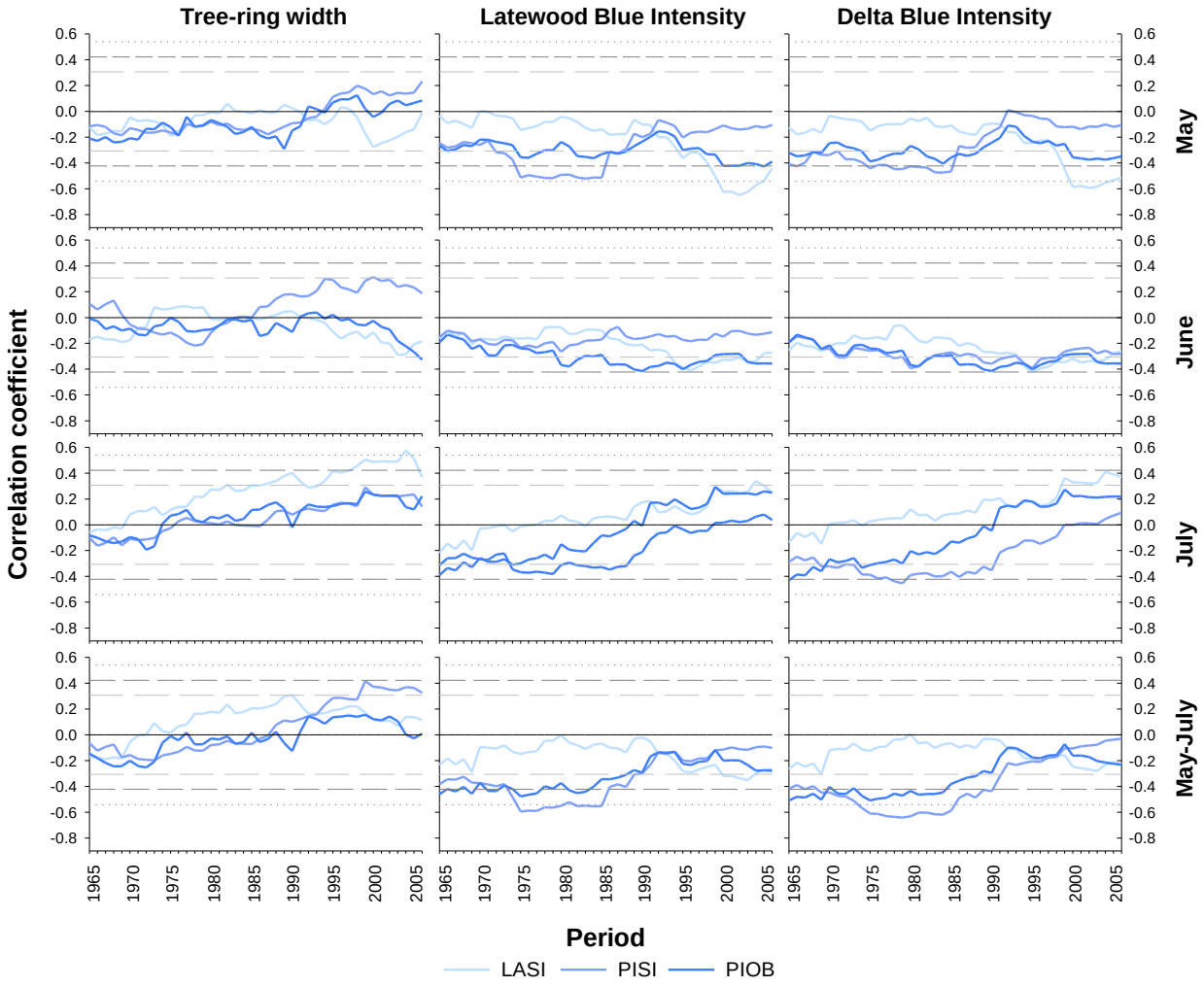

767

768 **Figure S5.** Thirty-year window moving correlations (1-year step) between tree-ring width, blue
769 intensity and delta blue intensity standard chronologies against May, June, July and May-July
770 precipitation over the 1951–2021 period. Long dashed, medium dashed and dotted horizonal
771 lines represent significant correlation at $p < 0.05$ and $p < 0.01$ and $p < 0.001$, respectively. LASI,
772 *Larix sibirica*; PISI, *Pinus sibirica*; PIOB, *Picea obovata*.

773

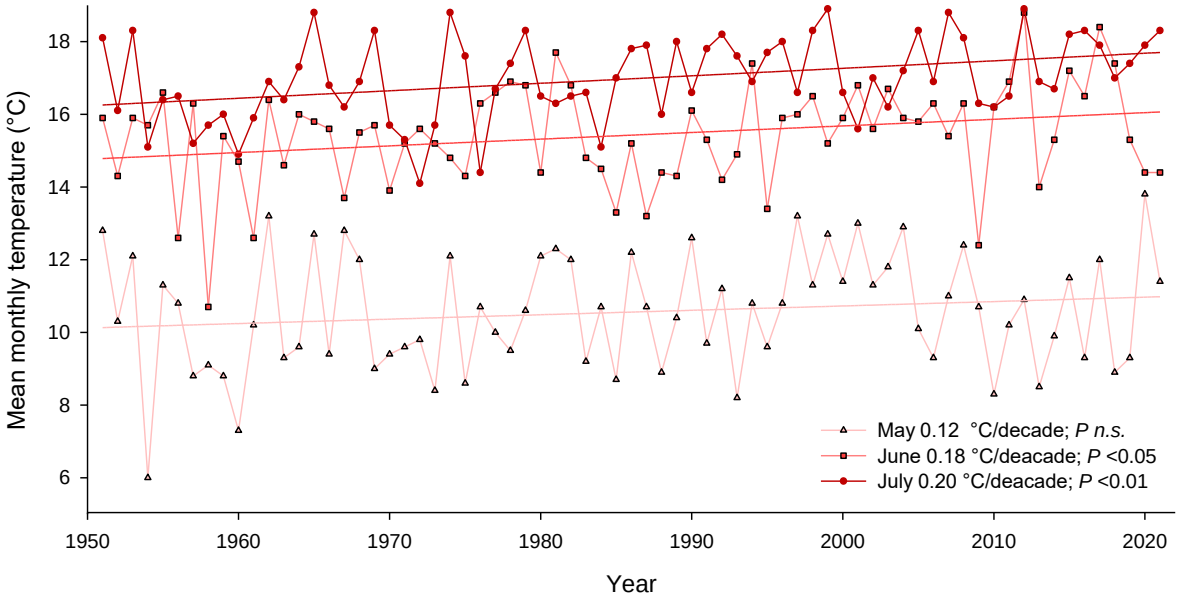

774

775 **Figure S6.** May, Ju ne and July temperatures trends for the 1951–2021 period.

776